Nuclear Science and Techniques (2025) 36:106
https://doi.org/10.1007/s41365-025-01691-7

Prompt fission neutron uranium logging (I): direct uranium quantification method theory

Yan Zhang[1,2] · Chi Liu[1,2] · Hai-Tao Wang[1,2] · Xiong-Jie Zhang[1,2] · Zhi-Feng Liu[1,2] · Rui Chen[1,2] · Jin-Hui Qu[1,2] · Ren-Bo Wang[1,2] · Bin Tang[1,2]

Received: 15 June 2024 / Revised: 15 June 2024 / Accepted: 10 July 2024 / Published online: 22 April 2025

Abstract

Prompt fission neutron uranium logging (PFNUL) is an advanced method for utilizing pulsed neutron bombardment of the ore layer and a fission reaction with uranium (^{235}U) to detect the transient neutrons produced by fission and then directly measure and quantify uranium; however, the stability and lifetime performance of pulsed neutron sources are the key constraints to its rapid promotion. To address these problems, this study proposes a PFNUL technique for acquiring the time spectrum of dual-energy neutrons (epithermal and thermal neutrons) from the upper and lower detection structures and establishes a novel uranium quantification algorithm based on the ratio of epithermal and thermal neutron time windows (*E*/*T*) via a mathematical-physical modeling derivation. Through simulations on well-logging models with different uranium contents, the starting and stopping times of the time window (Δt) for uranium quantification in the dual-energy neutron time spectrum are determined to be 200 and 800 μs, respectively. The minimum radius and height of the model wells are 60 and 120 cm, respectively, and the *E*/*T* values in the time window show an excellent linear relationship with the uranium content. The scale factor is $K_{E/T} = 1.92$ and $R^2 = 0.999$, which verifies the validity of the *E*/*T* uranium quantification algorithm. In addition, experiments were carried out in the Nu series of uranium standard model wells, and the results showed that under different neutron source yields, the *E*/*T*-based uranium quantification method reduced the relative standard deviation of the scale factor of the uranium content from 33.41% to 1.09%, compared with a single epithermal neutron quantification method. These results prove that the *E*/*T* value uranium quantification method is unaffected by the change in the neutron source yield, effectively improves the accuracy and service life of the logging instrument, and has great scientific and popularization value.

Keywords PFNUL · Uranium exploration · Pulsed neutrons · Neutron time spectrum

This work was supported by the National Natural Science Foundation of China (No. 42374226), Jiangxi Provincial Natural Science Foundation (Nos. 20232BAB201043, gpyc20240073, and 20232BCJ23006), Nuclear Energy Development Project (20201192-01), Fundamental Science on Radioactive Geology and Exploration Technology Laboratory (2022RGET20), and National Key Laboratory of Uranium Resource Exploration-Mining and Nuclear Remote Sensing (ECUT)(2024QZ-TD-09).

✉ Yan Zhang
yanzhang@ecut.edu.cn

✉ Bin Tang
tangbin@ecut.edu.cn

[1] National Key Laboratory of Uranium Resources Exploration-Mining and Nuclear Remote Sensing, East China University of Technology, Nanchang 330013, China

[2] Jiangxi Province Key Laboratory of Nuclear Physics and Technology, East China University of Technology, Nanchang 330013, China

1 Introduction

Nuclear power is one of the most promising ways to efficiently produce hydrogen on a large scale without emitting carbon dioxide. As the main fuel source for nuclear power generation, uranium ore is crucial to the development of the nuclear power industry [1]. Since the twenty-first century, countries worldwide have put forward actions to search for minerals and develop technological equipment for the intelligent exploration and development of minerals to provide scientific and technological support for energy conservation and emissions reductions.

Logging is an effective method for uranium exploration. The gamma (total) logging method originated in the field of petroleum logging in the 1930s and was applied to uranium logging development in the 1960s [2–6]. Gamma logging

belongs to the technique of "indirect uranium measurement" [7, 8], which detects gamma rays in drill holes to determine the activity of radium/radon daughters (nuclides), and then deduces the uranium content of the stratum according to the relationship of activity equivalence. When the mineralization environment and geological conditions change, the activity equivalence relationship is destroyed, the decay equilibrium relationship between uranium and radium/radon is broken, and the uranium content interpreted by logging deviates. Therefore, the industry standard for China's uranium mine gamma logging requires that no fewer than 30% of the samples taken from drill holes must be analyzed. The equilibrium relationship between uranium, radium, and radon should be examined accordingly, and the deviation of the uranium content interpretation should be corrected [9–11]. Therefore, uranium exploration in China is mainly realized via core chemical analyses combined with natural gamma logging technology. Natural gamma logging is simple in principle, but the accuracy of its quantitative interpretation is easily affected by the uranium–radium balance, radon radio gas, and thorium–potassium interference. This makes it difficult to satisfy the existing demand for uranium exploration, which causes shortcomings including high cost, low efficiency, and large errors in the quantification of uranium resources in the long term [12–14]. Therefore, there is an urgent need for a new theory, technology, and method of nuclear logging with high precision that can realize direct uranium measurement and downhole quantification of the uranium content in a formation.

In 1966, Allen and Tittle proposed a novel uranium logging technique called fission neutron logging. To elucidate the principle of the fission neutron uranium logging technique, single-velocity neutron diffusion equations simulating the geometry of a cylindrical borehole were solved, and a computer program was completed to address the entire analytical numerical problem [15, 16]. In 1972, Czubek analyzed the epithermal neutron time distribution, thermal neutron time distribution of ^{235}U slow fission, and fast neutron time distribution of ^{238}U slow fission, based on the epithermal neutron time distribution produced by ^{235}U prompt fission. When the background was almost zero, the stratigraphic epithermal neutron count rate was proportional to the uranium grade. A point-like pulsed neutron source in a uniform uranium-bearing sphere ore formation was modeled, and the formula for the response of the neutron detector to the epithermal neutron count rate was calculated, thus creating the basis of the methodology for the prompt neutron logging of uranium fission [17]. Renken [18] found significant variability between the epithermal neutron fluxes produced in formations with and without uranium and concluded that a logging method based on the time decay of epithermal neutrons has great potential. Simulations were performed for different uranium concentrations, and the results showed that the thermal neutron flux was independent of the uranium concentration. The Monte Carlo program TIMEX was applied in 1977 to simulate the signal contribution of the strata around the uranium fission prompt neutron logger to its epithermal neutron (0.414–454 eV) detector. The results showed that uranium ore at 0.3–0.5 m significantly contributed to the detector-received signal [18, 19]. Allen, Tittle, Czubek, Renken, and others provided a theoretical basis for the development of subsequent pulsed neutron uranium logging.

Since the 1970s, uranium logging methods based on pulsed neutron technology that can directly measure uranium (^{235}U) content without core sampling or interference from gamma rays of other radionuclides, such as thorium and potassium, have been the subjects of studies and experiments in which neutron logging technology was used for direct uranium measurement in the USA, Canada, Germany, and the former Soviet Union [20, 21]. All these are considered effective methods for uranium quantification through the collection of neutron time spectra. However, it is necessary to utilize neutron sources with ultrashort pulse widths and high yields, such as the pulsed neutron uranium logging system device ANHK-60 [22] developed by the All-Russian Research Institute of Automation (VNIIA) in Russia, which employs a D-T neutron generator with a pulse width of 1 μs and a single-pulse neutron yield of approximately 10^7 n/s; however, the lifetime of the generator is only 150 h.

Therefore, the stability and lifetime of the neutron source are key factors affecting the accuracy of uranium quantification, such as the change or fluctuation of the neutron flux in the neutron tube, which has a direct impact on the logging results [23]. Currently, the main approaches to improve the performance of neutron tubing are to use new materials, optimize the design to improve the lifetime, and use advanced control systems and feedback mechanisms in the logging instrument to stabilize the source neutron flux and reduce fluctuations through scale and automatic adjustments [24–26]. For example, Weibo Liu, Wen-Ting Guo, and other scholars improved the yield stability by optimizing both the pulse power supply of the neutron tube ion source and the target film preparation [27, 28]. Xiang-quan Chen and others improved the neutron yield stability by integrating the Kalman filter with the PID algorithm into the PLC [29]. The neutron yield of the generator was significantly stabilized at 1×10^8 n/s, and the relative standard deviation of the neutron yield during use was 0.82%. However, these neutron yield control techniques and correction methods have not solved the problem of the influence of the service lives of neutron tubes, which seriously restricts the popularization and application of PFNUL.

In this study, by exploring neutron transport theory, a dual neutron detector with upper and lower detection structures is proposed to realize the time spectrum detection of

epithermal neutrons (E) and thermal neutrons (T). The time window(Δ) is used to extract the effective information of the prompt neutrons produced by the uranium fission reaction, from which the quantitative equation of uranium based on the value (*E*/*T*) of epithermal and thermal neutrons is derived. The extraction of uranium fission neutron information is determined via simulations and experimental measurements. The *E*/*T* values within this time window show a good linear relationship with different uranium contents. Moreover, the uranium quantitative scale factor based on the *E*/*T* value is stable under different neutron yield conditions, demonstrating that the present method can eliminate the fluctuation of uranium quantification triggered by the fluctuation of the neutron source intensity, prolong the service lives of neutron tubes, and reduce the cost of using neutron uranium logging, which is of great significance for the popularization of neutron uranium logging [30–33].

2 Theory of direct uranium measurement methods for dual-energy neutron ratios

2.1 Theory of PFNUL

Figure 1 illustrates the principles of the PFNUL technique. The D-T neutron generator emits fast neutrons (called source neutrons) in a pulsed manner into the downhole formation, and these fast neutrons are slowed by elastic scattering, inelastic scattering, and other nuclear interactions with the formation rock. Fast neutrons are rapidly slowed down to epithermal neutrons (E) (epithermal neutron lifetime $\leq t_1$) and thermal neutrons (T), which stay in the stratum for a long time ($\leq 5000\,\mu s$) in the form of "thermal motion," during which they undergo radiative capture, fission, and other nuclear interactions with the nuclei of the material atoms, and are ultimately absorbed by the material (neutron fading). During a single pulsed neutron measurement cycle, the epithermal and thermal neutron time spectra in the formation are collected by an epithermal neutron detector and a thermal neutron detector, respectively, in which the slowed-down thermal neutrons are prone to undergo fission reactions with ^{235}U in the formation and thereby produce 2–3 uranium fission transient neutrons that prolong the epithermal neutron fading time ($\geq t_1$), as shown in Fig. 1b. This prolonged Δt portion of the epithermal neutrons is positively correlated with the uranium content.

2.2 Uranium quantification by epithermal neutrons

In 1972, Czubek proposed a novel direct uranium logging method that utilized a 14 MeV pulsed neutron source to continuously irradiate a uranium-bearing formation and measure the formation fission neutron time distribution at the end of the source neutron pulse [17]. Czubek theoretically demonstrated the feasibility of determining the uranium content by measuring the prompt fission epithermal neutron time spectrum resulting from the fission of the formation ^{235}U thermal neutron nucleus. Based on the energy, time, and space distributions of neutrons in the medium under isotropic pulsed neutron point source conditions, Czubek obtained the formula for the count rate of epithermal fission neutrons within the measurement time window by using an epithermal neutron detector record and derived that for an epithermal neutron detector with a determined performance, the epithermal neutron counts of the detector are only related to the source neutron yield Q when the parameters such as the measurement timing of the logging system, formation uranium content q_u, formation density ρ, and formation neutron characteristic function $f(t_s, \Sigma_a)$ are fixed:

$$\text{Epi.Count} = K_E \cdot Q\rho q_u \cdot f(t_s, \Sigma_a) \tag{1}$$

where Epi.Count is the count of epithermal neutrons in the measurement time window, K_E is the scale factor for the system and denotes the coefficient of proportionality between the epithermal neutron counts and uranium content q_u, Σ_a is the macroscopic thermal neutron absorption cross section

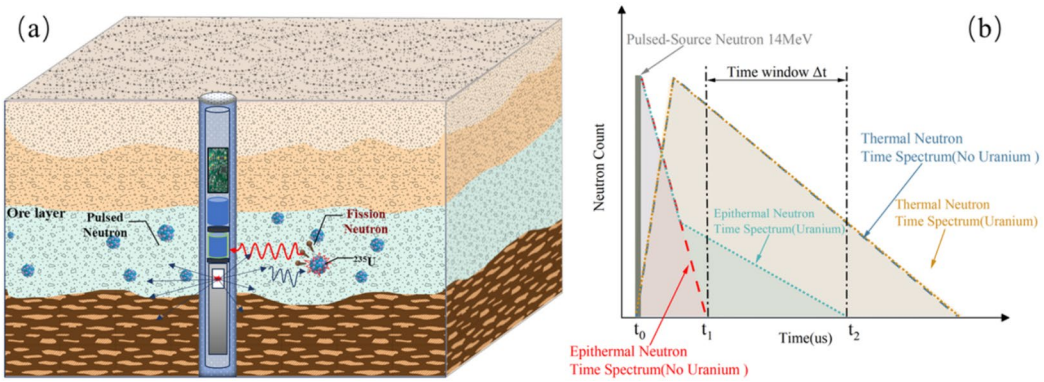

Fig. 1 (Color online) **a** Principle of PFNUL. **b** Epithermal and thermal neutron time spectrum for no-uranium and uranium cases

of the formation, and t_s is the average slowing time of the fast neutrons. However, a single epithermal neutron time spectrum is susceptible to fluctuations in the neutron source yield.

2.3 Uranium quantification of the epithermal neutron–thermal neutron ratio (*E*/*T*)

The epithermal fission neutron counting model proposed by Czubek in 1972 is an absolute method of uranium content quantification that requires compensatory measurements of parameters, including the source neutron yield (Q), formation density (ρ), and macroscopic thermal neutron absorption cross section (Σ_a). In 1978, Givens et al. proposed a relative uranium content measurement method in which a thermal neutron detector was added to the logging equipment to measure the formation thermal neutron time spectrum. The uranium content was quantified by measuring the ratio of the uranium fission neutron counts to the thermal neutron counts of the formation [34]. The epithermal fission neutron counts versus thermal neutron counts (Ther.Count) contributed by the ^{235}U thermal neutron nuclear fission reaction within the detector measurement timeframe are given by Eq. (2):

$$\begin{cases} \text{Epi.Count} = \varepsilon_{\text{epi}} N_u \sigma_{fU} g(S, \Sigma_a, t_b, t_c) f(\Sigma_a, t_c) \\ \text{Ther.Count} = \varepsilon_{\text{ther}} g(S, \Sigma_a, t_b, t_c) f(\Sigma_a, t_c) \end{cases} \tag{2}$$

where ε_{epi} is the detection efficiency of the epithermal neutron detector, N_u is the ^{235}U atomic number density of the formation, σ_{fU} is the ^{235}U nuclear fission reaction cross section, $g(S, \Sigma_a, t_b, t_c)$ is the thermal neutron flux density of the formation at the end of the waiting time t_b, S is the source neutron yield, Σ_a is the macroscopic thermal neutron absorption cross section of the formation, $f(\Sigma_a, t_c)$ is the thermal neutron flux at measurement time t_c, and $\varepsilon_{\text{ther}}$ denotes the detection efficiency of the thermal neutron detector.

The $g(S, \Sigma_a, t_b, t_c)$ term represents the thermal neutron source that causes the ^{235}U thermal neutron nuclear fission reaction, and any factor affecting the thermal neutron flux of the formation affects the epithermal fission neutron flux. The macroscopic thermal neutron absorption cross section of the formation can affect its thermal neutron flux. To correct the influence of the formation parameters and other factors on the thermal neutron flux of the formation, Givens et al. proposed an epithermal neutron–thermal neutron counting model. The model equations contain the same thermal neutron correlation terms. Hence, the influencing factor correlation terms of the formation can be eliminated by the ratio method $g(S, \Sigma_a, t_b, t_c)$ and $f(\Sigma_a, t_c)$ on the epithermal neutron flux counting. Moreover, the relationship between the epithermal fission neutron-thermal neutron counting ratio and ^{235}U atomic number density of the stratum is obtained via the ratio method, as shown in Eq. (3):

$$\frac{\text{Epi.Count}}{\text{Ther.Count}} = \frac{\varepsilon_{epi} N_u \sigma_{fU}}{\varepsilon_{\text{ther}}} \tag{3}$$

In logging equipment, Givens et al. arranged thermal neutron and epithermal fission neutron detectors with equal source spacing to ensure that the thermal neutron correlation terms $g(S, \Sigma_a, t_b, t_c)$ and $f(\Sigma_a, t_c)$ at the positions of the thermal neutron and epithermal neutron detectors in Eq. (2) were equal. However, in practical engineering applications, an equal source spacing thermal neutron and epithermal fission neutron detector arrangement is not achievable, owing to the limitation of the spatial location. Therefore, the authors proposed the use of a double neutron detector with upper and lower structures for the acquisition of the time spectra of epithermal neutrons (E) and thermal neutrons (T), respectively, as shown in Fig. 1a, and constructed the *E*/*T* values to eliminate the fluctuating effects of the neutron source yields. During the life cycle of a neutron, thermal neutrons are prone to fission with ^{235}U within the medium and produce uranium fission transient neutrons, thereby prolonging the epithermal neutron fading time, as shown in Fig. 1b, which is the theoretical basis for detecting the occurrence of uranium fission, as well as for uranium ore quantification using pulsed neutron logging. According to the theory of uranium fission, in a homogeneous medium (saturated ore layer), at any time t after all the primary pulsed neutrons have been slowed down to thermal neutrons (denoted as the t_1 moment), the total number of existing epithermal neutrons in the medium $n_E(t)$ is proportional to the total number of existing thermal neutrons $n_T(t)$ versus the uranium content (or ^{235}U content):

$$\frac{n_E(t)}{n_T(t)} = \frac{n_E(t_1) \cdot e^{-(t-t_1)/\tau_E}}{n_T(t_1) \cdot e^{-(t-t_1)/\tau_T}} = K_U \cdot q_u \tag{4}$$

Equation (4) shows that after the slowing down of primary neutrons to thermal neutrons, the total amount of existing epithermal neutrons $n_E(t)$ and thermal neutrons $n_T(t)$ in the homogeneous medium decay according to the negative exponential law, i.e., the time spectrum of epithermal neutrons and thermal neutrons at this time period, is the decay time spectrum [35]. The decay rates are described by $1/\tau_E$ and $1/\tau_T$ (τ_E and τ_T are the time constants for the fading times of epithermal and thermal neutrons, and their values are closely related to the stratum rock, drilling medium, and neutron nuclear interaction ability). Moreover, K_U denotes the positive coefficient of the ratio of the total amounts of existing epithermal and thermal neutrons in the formation rock to the uranium content q_u after the moment of t_1. Thus, determining the time window parameters t_1 and t_2 shown in Fig. 1b is critical; otherwise, the epithermal neutrons produced by the

neutron source affect the accuracy of uranium quantification, as discussed below.

If a logging probe measures the double neutron time spectra of $n_E(t)$ and $n_T(t)$ at a certain measurement point along the well axis, then the epithermal neutron attenuation at Δt is $N_E(\Delta t)$, the thermal neutron attenuation is $N_T(\Delta t)$, and the ratio of the two attenuations is called the "epithermal/thermal" (E/T) value. The detected epithermal neutron attenuation $N_E(\Delta t)$ and thermal neutron attenuation $N_T(\Delta t)$ come from the upper and lower structural distributions of ^{3}He orthotropic technology tubes, respectively.

$$\begin{cases} N_E(\Delta t) = \eta_E \int_{t_1}^{t_2} n_E(t)dt = \eta_E \cdot n_E(t_1)\tau_E(1 - e^{-\Delta t/\tau_E}) \\ N_T(\Delta t) = \eta_T \int_{t_1}^{t_2} n_T(t)dt = \eta_T \cdot n_T(t_1)\tau_T(1 - e^{-\Delta t/\tau_T}) \end{cases} \quad (5)$$

Hence, the E/T value is proportional to the formation rock formation.

$$E/T(\Delta t) = \frac{N_E(\Delta t)}{N_T(\Delta t)} = K_{E/T} \cdot q_u \quad (6)$$

In Eqs. (5) and (6), η_E is the effective detection efficiency of epithermal neutron attenuation, which indicates the ratio of detected epithermal neutron attenuation to the actual epithermal neutron attenuation; similarly, η_T is the effective detection efficiency of thermal neutrons, and $K_{E/T}$ is the conversion factor that indicates the positive coefficient of the E/T to the uranium content q_u. Moreover, this conversion factor is the covariate determined by the factors of logging instrument, stratum rock, drilling medium, etc. Once the logging instrument, formation rock, and drilling medium are fixed (particularly the logging instrument), $K_{E/T}$ remains constant.

In the above equation, $K_{E/T}$ is considered the known variable, $E/T(\Delta t)$ is the measured variable, and q_u is the variable to be solved. For this reason, it is necessary to construct accurate uranium model wells that are similar to field wells in terms of lithological structure, material composition, and medium in the wells and then use the PFNUL instrument to scale the model wells with known uranium contents to determine the derived $K_{E/T}$, carry out actual field logging, and then substitute it into Eq. (6) to determine the uranium content of the field wells q_u. Therefore, determining the dimensional parameters of the uranium model wells is also important in this study.

In Eqs. (6), $E/T(\Delta t)$ is added to the epithermal neutrons, thermal neutrons, and fading time correction, which are attributable to the negative exponential decay law of epithermal neutrons and thermal neutrons, respectively, as well as the decay time spectrum of negative exponential fitting in finding the value of τ_E,τ_T. Because the values of τ_E and τ_T in a homogeneous medium are relatively stable, the fading time correction coefficient can also be set to the value of $K_{E/T}$. Moreover, when the t_2 value is large, the count rate of the tail of the epithermal neutron time spectrum has a large statistical rise and fall (which may also include the uranium fission delayed neutrons), when the frequency of the pulsed neutron emission reaches or exceeds 1000 Hz, then it must be $\leq$ 1000 μs. Therefore, it is recommended that the value of Δt be set between 600 and 1000 μs.

The advantages of this method lie in the following: extracting the secondary neutron extinction law from the epithermal neutron time spectrum and the primary neutron slowing law from the thermal neutron time spectrum to select the appropriate time window parameters, define the "epithermal/thermal" ratio based on the two-neutron time spectrum, and construct a real-time algorithm for uranium ore quantification. Thus, the "direct uranium measurement" and quantification via the prompt neutron logging of uranium fission was realized.

3 Theoretical validation of the proposed method

3.1 Time windows (Δt)

In this study, the Monte Carlo method was used to establish a model of a PFNUL instrument with a ratio of epithermal neutrons to thermal neutrons and a model of cylindrical saturated uranium ore with reference to the actual model [36–38], as shown in Fig. 2a. Among them, the outer diameter of the probe tube was 5.5 cm, and the length of the probe tube was 284 cm. The pulsed neutron source was a 14 MeV D-T pulsed neutron source with a pulse width of 10 μs, and the two ^{3}He detectors were distributed in an upper and lower structure, with the upper ^{3}He detector wrapped with 1 mm cadmium and 4 mm polyethylene for epithermal neutron (energy range of 0.7–1000 eV) time spectrum acquisition and the lower ^{3}He detector. The neutron source and center of the epithermal neutron detector had a source distance of 15.15 cm, and the neutron source and center of the thermal neutron detector had a source distance of 43.7 cm. The uranium content of the stratum was set to be 0%, 0.0280%, 0.0684%, and 0.0982%, respectively, and the results of the simulated time spectrum are shown in Fig. 2b.

Figure 2b shows that the thermal neutron time spectra are the same in both the uranium-bearing and non-uranium-bearing layers. This means that regardless of whether the ore layer contains uranium, as long as the formation rocks, drilling conditions, and other factors remain unchanged, the difference in the macroscopic absorption cross section of the thermal neutrons is small (almost the same). At any

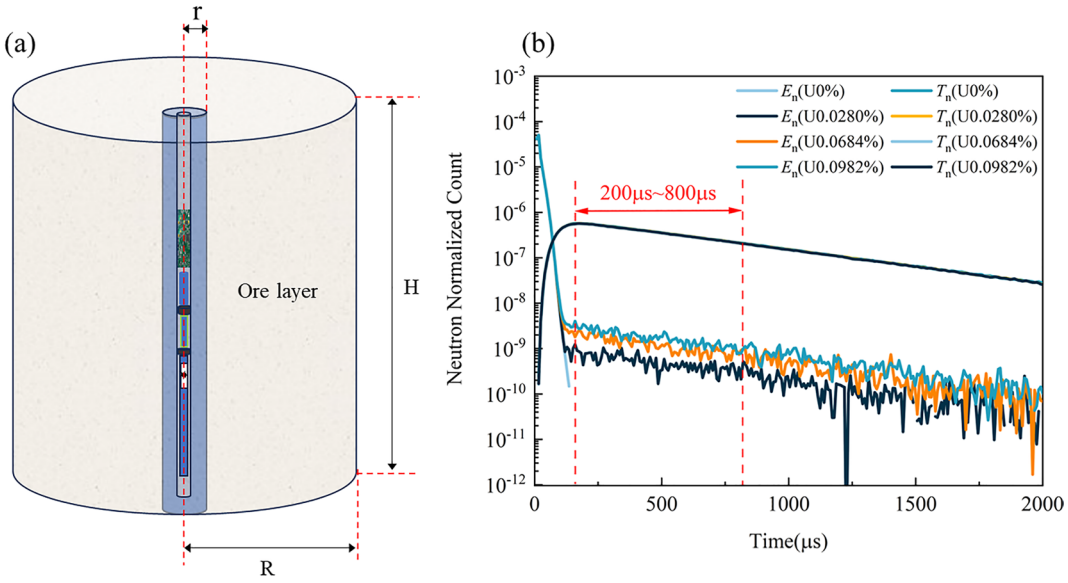

Fig. 2 (Color online) **a** Uranium logging model. **b** Time spectrum of epithermal and thermal neutrons and Δt for the uranium signature information acquisition, where E_n denotes the normalized counts of the epithermal neutron time spectrum and T_n denotes the normalized counts of the thermal neutron time spectrum

time ($t \geq t_1$), the number of existing thermal and epithermal neutrons in the formation rocks with a law of change over time is a negative exponential decay function. In the epithermal neutron time spectrum of the pure sandstone model (0% uranium content), there are no counts after 200 μs, and all neutrons produced by the neutron source are converted to thermal neutrons after 200 μs, which is the value of t_1 in Eqs. (5). Then, in the epithermal neutron time spectrum with uranium contents of 0.0280%, 0.0684%, and 0.0982%, respectively, the epithermal neutron counts after 200 μs are all produced by the decelerated production of fast neutrons from the uranium fission reaction, and the number is related to the uranium content. When the time is after 800 μs, the epithermal neutron counts in the model of uranium-containing layers are less distinguishable, and the statistical rise and fall of the epithermal neutrons after this moment are larger and may also be credited to the uranium fission slow-generating neutrons. Hence, the t_1 and t_2 of the uranium characterization information acquisition for the *E*/*T* value are taken to be 200 and 800 μs, respectively.

3.2 Standard model wells

The ideal standard model well size should be as large as possible, beyond the effective detection range. Therefore, the determination of the appropriate height (*H* in Fig. 2a) and radius (*R* in Fig. 2a) of the standard model is important. Using the Monte Carlo method, based on the aforementioned neutron logger model, the size of the mineral layer model gradually increases with the detector performance, source term, and formation medium unchanged. Moreover, the appropriate height and diameter of the standard model well are determined according to the variation of the *E*/*T* value. Figure 2a shows the model. Considering that the neutron counts measured by the uranium fission neutron logger are affected by the uranium content of the formation and the size of the borehole radius *r*, we set the uranium content of the formation to be 0.0280%, 0.0684%, and 0.0982% and the radius of the borehole to be 3, 7, 11, and 16.5 cm, respectively. Then, we change the model height and simulate the uranium fission neutron logging *E*/*T* values using the Monte Carlo software. The height of the saturated uranium model is determined based on the stability of the *E*/*T* value. Under the same conditions, the radius of the model was changed, and Monte Carlo software was used to simulate the *E*/*T* value. The radius of the saturated uranium logging model was determined according to the stability of the *E*/*T* value. Figure 3 shows the simulation results.

Figure 3a–c shows the changes in the *E*/*T* value with the model height. The results show that the *E*/*T* value detected by the uranium fission transient neutron logger increases with an increase in the logging model radius *R*. However, after the model radius reaches a certain value, the *E*/*T* value does not change significantly with a further increase in the model height. In addition, with a smaller the borehole radius *r*, changes of the model radius *R* will lead to more drastic changes of the *E*/*T* value. The changes in the *E*/*T* value are relatively insignificant with changes in the model height when the borehole radius exceeds 7 cm. Thus, the simulation

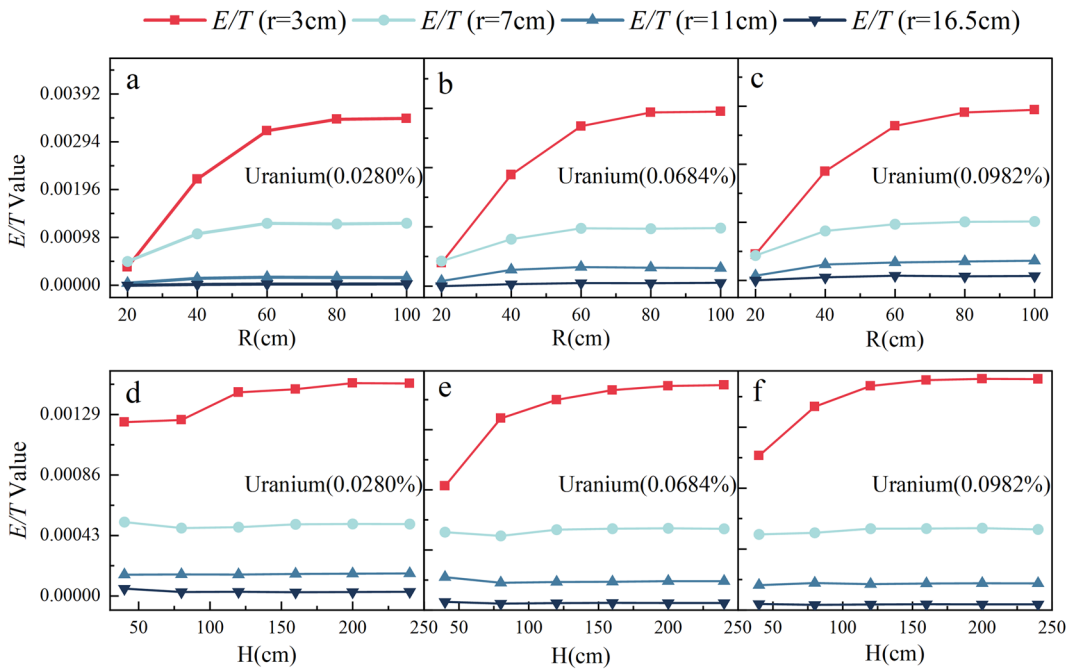

Fig. 3 (Color online) **a–c** Simulation results of the saturated uranium model radius *R*. **d–f** Simulation results of the saturated uranium model height *H*

results show that for the radius *R* of the saturated ore layer, $R \geq 60$ cm.

The changes in the *E*/*T* value with respect to the model radius are shown in Fig. 3d–f. The results show that with an increase in the logging model height *H*, the *E*/*T* value detected by the PFNUL instrument is more significantly increased when the borehole radius is 3 cm. In contrast, the changes in the *E*/*T* value with changes in the model height are relatively insignificant when the borehole radius exceeds 3 cm. The number of *E*/*T* values does not change significantly with an increase in the model height and is less affected by the borehole radius *r*. After the model reached a certain height, the number of *E*/*T* values did not change significantly with an increase in the model height and was less affected by the borehole radius *r*. Therefore, the simulation results show that $H \geq 120$ cm for the height of the saturated layer.

After the simulation, it was determined that the height of the saturated uranium ore model $H \geq 120$ cm, radius $R \geq 60$ cm, and measurement results of the neutron detector under the model of the ore layer of this size were the same as those of the infinite ore layer.

The experimental model used in this experiment was the Nu series of the sandstone-type uranium ore standard model wells constructed by the Airborne Survey and Remote Sensing Center of Nuclear Industry (ASRSCNI), as shown in Fig. 4a. Models Nu-1, Nu-2, and Nu-3 are uranium-bearing models (red) with uranium contents of 0.0281%, 0.0685%, and 0.0983%, respectively. The Nb-4 model, in which the uranium taste is much lower than the boundary taste, is defined as a pure sandstone model without uranium and is a background count test model (green). The borehole radius *r* of each uranium cylinder model drill hole is 9 cm, the model radius *R* is 70 cm, and the height is 180 cm. Moreover, a 90-cm-thick concrete roof is set on the model, a 30-cm-thick concrete base is set under the model, and extension holes are set below the base at a depth of 260 cm. The size of the model meets the requirements of the saturation model. Figure 4b shows the PFNUL instrument, which contains two sets of ^{3}He tubes in the well-logging instrument, a polyethylene neutron moderating material wrapped around the epithermal neutron detector, a cadmium metal skin wrapped around the moderating material, a high-voltage power supply for the detector, a preamplifier, shaping and screening circuitry, a pulse counter to record the output signals from the dual neutron detector, a time spectrum analysis, and cache circuits to record the output signals of the dual neutron detectors.

3.3 Simulated scale factor

According to the simulation results, to find the conversion relationship between the *E*/*T* value and uranium content, considering the reduction of the influence of the statistical rise and fall on the counting results, the simulated time spectra with different uranium contents (pure sandstone,

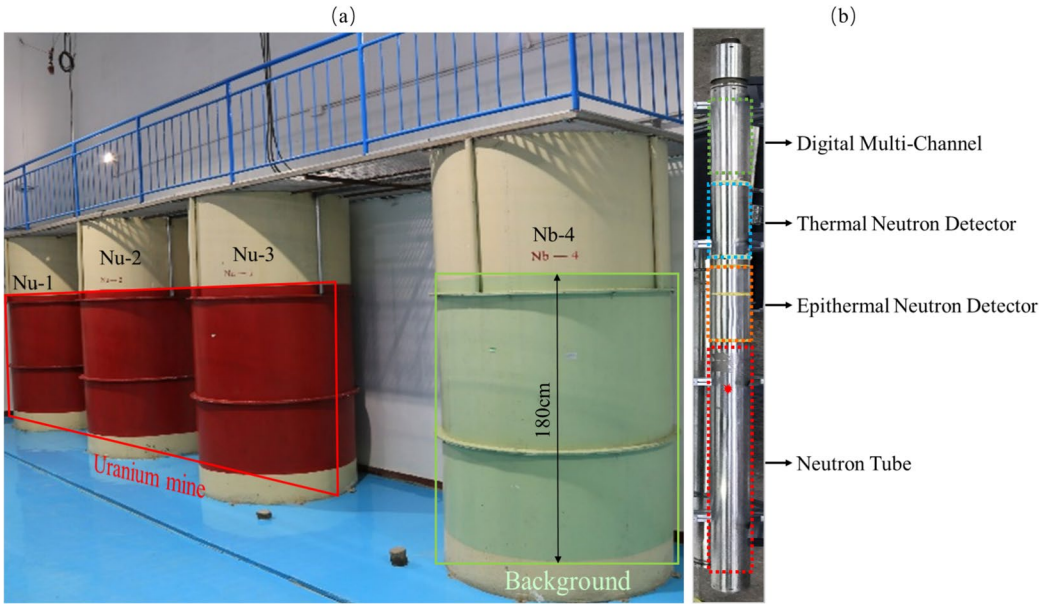

Fig. 4 (Color online) **a** Standard model wells for Nu series sandstone-type uranium mines. **b** PFNUL instrument

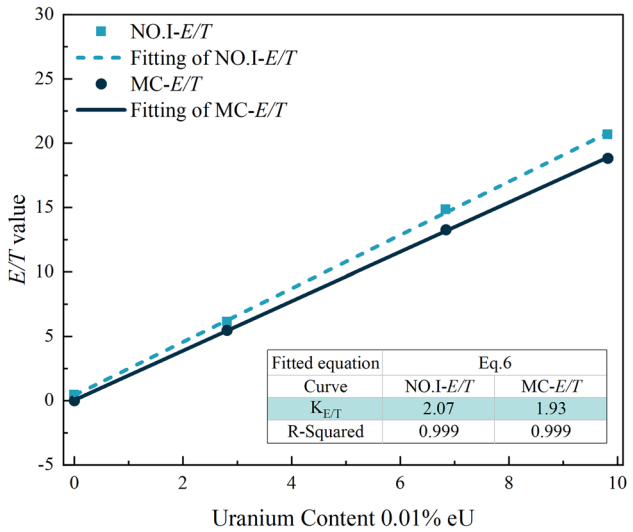

Fig. 5 (Color online) PFNUL simulation scale curve

0.0280%, 0.0684%, and 0.0982%) are taken as the starting and ending times of 200–800 μs, and the total counts of epithermal and thermal neutrons and neutrons are calculated. The scale curve of the uranium fission prompt neutron instrument for this study was compared with the *E*/*T* value curve calculated from the experimental raw data, as shown in Fig. 5.

Figure 5 shows a comparison of the simulated correspondence between the uranium content and *E*/*T* value and the experimental results, which can be fitted using Eqs. (6). The conversion coefficient of the simulated results of the uranium content and *E*/*T* value $K_{E/Tmc} = 1.93(0.01\%eU/cps)$ exhibit a fit of $R^2 = 0.999$, and the same can be obtained from the experimental data with a conversion coefficient of $K_{E/T} = 2.07(0.01\%eU/cps)$. The deviation of simulation and experiment comparison is 7.25%. The simulation results are in line with the principle of PFNUL, based on the ratio of epithermal to thermal neutrons.

4 Neutron yield impact

4.1 Time spectra of different neutron yields

Owing to the consumption of the experiments and tritium, the neutron yield of the D-T neutron tube changed with use. To investigate the effect of the neutron yield on the accuracy of uranium quantification, four sets of experiments were conducted, in which the neutron intensity of the D-T neutron source was varied slightly. The neutron source intensity was based on Experiment No. I, and the relative intensities of the neutron sources of the remaining experiments were calculated, as shown in Table 1.

As shown in Fig. 6, four sets of neutron time spectra and epithermal neutron time spectra were measured using a logging instrument at different neutron source intensities in the Nu series sandstone uranium logging model (Fig. 4a) from the ASRSCNI.

Table 1 Neutron relative intensities of the D-T neutron sources in the experiments

Measurement ID	D-T pulsed neutron source flux	Neutron source strength
I	62068150	1
II	27816560	0.45
III	65526101	1.06
IV	52639004	0.85

4.2 Effect of the neutron source strength on the epithermal neutron counts and *E*/*T* values

As listed in Table 1, the relative intensities of the neutron sources in the four experiments were not equal. Figure 7 shows the changes in the *E*/*T* values and epithermal neutron counts measured in the standard uranium mine model with the changes in the intensity of the neutron sources in the four experiments.

Figure 7 shows that different neutron source intensities have a significant influence on the counts of epithermal neutrons, which results in significant changes in the epithermal neutron counts; however, there is no significant change in the *E*/*T* values under different neutron source intensities. The relative standard deviation (RSD) was used to measure the stability of the *E*/*T* value and epithermal neutron counts under different neutron source intensities [39, 40]. The calculation formula is as follows:

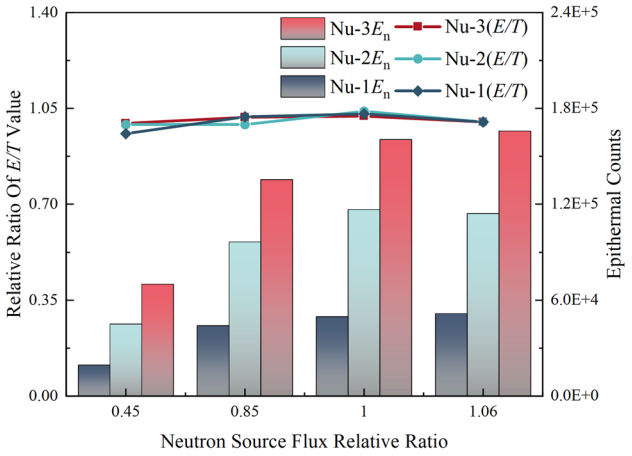

Fig. 7 (Color online) Variation of *E*/*T* values and epithermal neutron counts

$$\mathrm{RSD} = \frac{\sqrt{\frac{\sum_{i=1}^{n}(x_i-\bar{x})^2}{n-1}}}{\bar{x}} \times 100\% \tag{7}$$

where x is the epithermal neutron count or the *E*/*T* value for the same uranium model, i denotes the corresponding experimental group, and $\bar{x}$ is the mean value.

The RSD values of the epithermal neutron counts and *E*/*T* values for different uranium contents in each group of experiments were calculated, as shown in Table 2. The maximum value of the standard deviation of the counts of epithermal neutrons reaches 36.32%, whereas the relative standard deviation of the *E*/*T* values is relatively stable, with a maximum value of only 3.2%, proving that the fluctuation

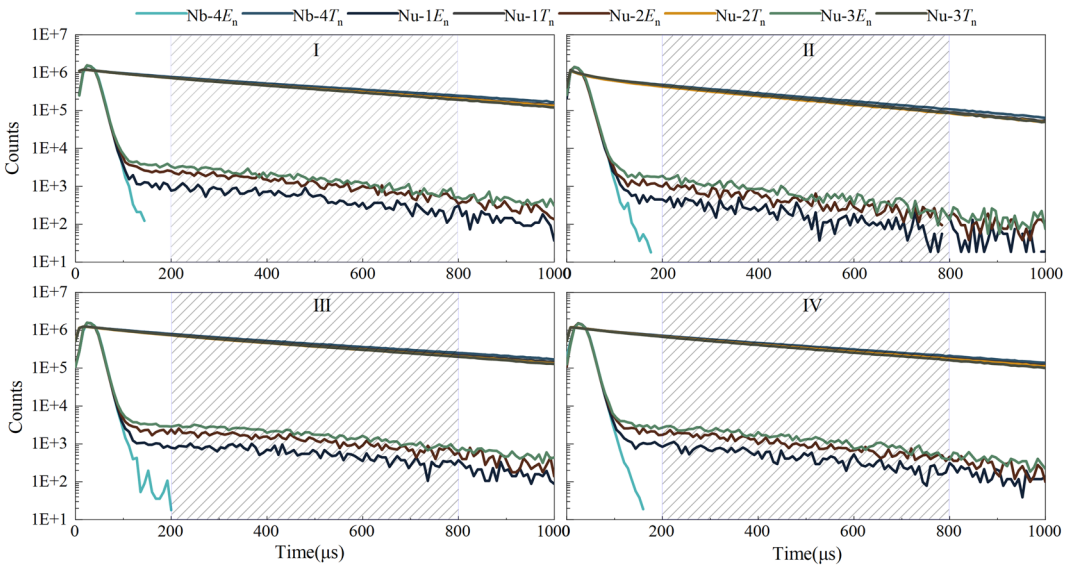

Fig. 6 (Color online) **I** Neutron time spectrum test results of Experiment I. **II** Neutron time spectrum test results of Experiment II. **III** Neutron time spectrum test results of Experiment III. **V** Neutron time spectrum test results of Experiment IV

Table 2 RSD of epithermal neutron count values and *E/T* values for different relative intensities of neutron sources

Experiment	Epithermal counts			*E/T* values		
ID	Nu-1	Nu-2	Nu-3	Nu-1	Nu-2	Nu-3
I	49676	114001	160359	6.12	14.83	20.67
II	19314	45006	70024	5.69	14.14	20.14
III	51611	116601	165723	5.94	14.27	20.23
IV	44123	96532	135385	6.06	14.14	20.58
RSD	36.23%	35.72%	33.07%	3.20%	2.29%	1.27%

of the neutron yield has a large impact on the counts of epithermal neutrons, whereas its impact on the *E/T* values is small.

4.3 Variation of the scale factor for different neutron source intensities

Based on the experimental data, we calculated the epithermal neutron counts for different neutron source intensity test data with different uranium contents within a time of 200–800 μs, and we linearly fitted the relationship between the epithermal neutron counts and uranium content, as shown in Fig. 8a. The figure clearly shows that the epithermal neutron counts and uranium content have a good linear relationship; however, the epithermal neutrons of the same uranium content change with the relative intensity change of the neutron source. The fluctuation of neutron tube production in the process of uranium measurement has a greater impact on the results of the counting of epithermal neutrons, which directly affects the uranium measurement accuracy. After the time normalization of the experimental time spectrum, the counts of epithermal and thermal neutrons from 200–800 μs for different uranium contents in the four sets of experimental data were calculated. Additionally, the corresponding *E/T* values were calculated. Finally, the corresponding relationship curves were obtained based on the linear fitting of the *E/T* values to the uranium content, as shown in Fig. 8b).

The linear fitting results showed that the uranium quantitative scale factors K_E based on epithermal neutron counting without relevant correction factors in the four sets of experiments conducted were 6896.2, 16110.6, 16381.2, and 13434.1. The RSD value was 33.41%, and the uranium quantitative scale factors $K_{E/T}$ based on the *E/T* value were 2.07, 2.02, 2.03, and 2.05, respectively. The RSD value was 1.09%. It has been proven that the E/T-based uranium quantification method based on the double neutron time spectrum can effectively and accurately analyze uranium quantification and that the scale factor is not affected by the neutron tube yield, which can effectively improve the service life of the neutron logging instrument.

5 Conclusion

In this research, based on the prompt fission reaction between uranium and neutrons, a PFNUL method with an up and down detection structure is proposed. Moreover, the secondary neutron fading law is extracted from the epithermal neutron time spectrum, the primary neutron slowing law

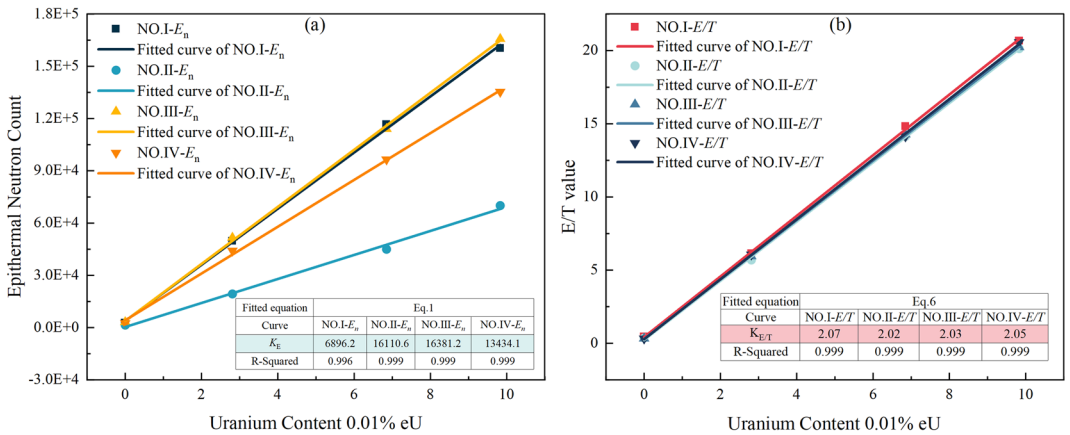

Fig. 8 (Color online) **a** Fitted curves of the epithermal neutron counts versus the uranium content. **b** Fitted curves of the *E/T* values versus the uranium content for four groups of experiments

is extracted from the thermal neutron time spectrum, and a uranium quantification algorithm based on the *E*/*T* value of the dual neutron time spectrum is subsequently proposed, thus realizing the "direct measurement of uranium" and uranium quantification. Via Monte Carlo simulations, a model radius $R \geq 60$ cm and height $H \geq 120$ cm were determined for the saturated neutron uranium logging model, and the starting and ending times of the time window (Δt) were 200 and 800 μs for t_1 and t_2, respectively. The Monte Carlo simulation results showed that the *E*/*T* value had a strong positive relationship with the uranium content, with a scale factor of 1.93 and an R^2 value of 0.999. Finally, in the saturated uranium model, experiments were carried out using the saturated uranium model to verify the positive relationship between the *E*/*T* value and uranium content, and the experimental results were compared with different neutron source intensities in the standard model of uranium ore. These results prove that the method can maintain the stability of the *E*/*T* value under different neutron source intensities and reduce the RSD of the scale factor of the uranium content from 33.41% to 1.09%, compared with the single method of quantification of epithermal neutron uranium ore. Hence, effectively eliminating the influence of fluctuations in neutron source yields, ensuring the accuracy of uranium quantification in the logging process, extending the service life of neutron tubing, and reducing the cost of neutron uranium logging are of great significance for the popularization and application of neutron uranium logging.

Author contributions All authors contributed to the study conception and design. Material preparation, data collection and analysis were performed by Yan Zhang, Chi Liu, Hai-Tao Wang, Xiong-Jie Zhang, Zhi-Feng Liu, Jin-Hui Qu, Ren-Bo Wang, and Bin Tang. The first draft of the manuscript was written by Yan Zhang and Chi Liu and all authors commented on previous versions of the manuscript. All authors read and approved the final manuscript.

Data availability The data that support the findings of this study are openly available in Science Data Bank at https://cstr.cn/31253.11.sciencedb.09149 and https://doi.org/10.57760/sciencedb.09149

Declarations

Conflict of interest The authors declare that they have no Conflict of interest.

References

1. H.R. Zhang, Y. Zhang, W.X. Hu et al., Simulation study of uranium content in uranium yellow cake using the active multiplicity method. Nucl. Tech. (in Chinese) **47**, 020202 (2024). https://doi.org/10.11889/j.0253-3219.2024.hjs.47.020202
2. L.G. Howell, A. Frosch, Gamma-ray well-logging. Geophysics **4**, 106–114 (1939). https://doi.org/10.1190/1.1440486
3. J.S. Wahl, Gamma-ray logging. Geophysics **48**(11), 1421–1560 (1983). https://doi.org/10.1190/1.1441436
4. R.A. Broding, B.F. Rummerfield, Simultaneous gamma ray and resistance logging as applied to uranium exploration. Geophysics **20**(4), 745–961 (1955). https://doi.org/10.1190/1.1438193
5. P.G. Killeen, Borehole logging for uranium by measurement of natural γ-radiation. Int. J. Appl. Radiat. Isot. **34**, 231–260 (1983). https://doi.org/10.1016/0020-708X(83)90128-X
6. R.L. Caldwell, Nuclear logging methods. Radioisotopes **17**(4), 171–185 (1968). https://doi.org/10.3769/radioisotopes.17.4_171
7. R. Chen, Y.L. Cheng, H.T. Wang et al., A union neutron-gamma logging method for determination of uranium-radium disequilibrium coefficient. Nucl. Technol. Radiat. Prot. **35**(2), 103–108 (2020). https://doi.org/10.2298/NTRP2002103C
8. L. Zhang, H.W. Yu, T. Li et al., Improved formation density measurement using controllable D-D neutron source and its lithological correction for porosity prediction. Nucl. Sci. Tech. **33**, 3 (2022). https://doi.org/10.1007/s41365-022-00988-1
9. B. Tang, Y.P. Wu, X.J. Zhang et al., Direct uranium quantitative detection in high precision γ-logging by 1.001 MeV 234mPa γ -ray. Nucl. Tech. (in Chinese) **35**(10), 745–750 (2012)
10. C. Lin, Y.Q. Chen, Q.W. Zhang et al., Calculation of U, Ra, Th and K contents in uranium ore by multiple linear regression method. Nucl. Tech. (in Chinese) **6**, 369–371 (1991)
11. F. Zhang, L.L. Tian, Research development and tendency of controllable neutron and X-ray source well logging technology. J. Isot. **32**(3), 133–150 (2019). https://doi.org/10.7538/tws.2019.32.03.0133
12. T. Marchais, B. Pérot, C. Carasco et al., Low-resolution gamma spectrometry of uranium ores to determine U concentration and U/Rn imbalance. IEEE Trans. Nucl. Sci. **69**(4), 761–767 (2022). https://doi.org/10.1109/TNS.2021.3129343
13. P. Sahu, D.P. Mishra, D. Panigrahi et al., Radon emanation from low-grade uranium ore. J. Environ. Radioact. **126**, 104–14 (2013). https://doi.org/10.1016/j.jenvrad.2013.07.014
14. W.M. Yin, H.Z. Liu, B. Tang et al., Determination of uranium-radium equilibrium coefficient of uranium ore sample using characteristic peaks in γ-ray spectrum. At. Energy Sci. Technol. **44**(7), 769–772 (2010). https://doi.org/10.7538/yzk.2010.44.07.0769. (**in Chinese**)
15. C.W. Tittle, L.S. Allen, Theory of neutron logging. II. Geophysics **31**, 214–224 (1961). https://doi.org/10.1190/1.1439737
16. L.S. Allen, C.W. Tittle, W.R. Mills, Dual-spaced neutron logging for porosity. Geophysics **32**, 60–68 (1967). https://doi.org/10.1190/1.1439857
17. J.A. Czubek, Pulsed neutron method for uranium well logging. Geophysics **32**(1), 160–173 (1970). https://doi.org/10.1190/1.1440244
18. J.H. Renken, Determination of the probing distance in pulsed-neutron uranium logging experiments. Nucl. Sci. Eng. **63**(3), 330–335 (1977). https://doi.org/10.13182/NSE77-A27044
19. J.H. Renken, Comparison of predicted signals from the delayed fission neutron and prompt fission neutron uranium logging methods. J. Appl. Phys. **49**(2), 6153–6159 (1978). https://doi.org/10.1063/1.324538
20. X.G. Wang, D. Liu, F. Zhang, Development of pulsed neutron uranium logging instrument. Rev. Sci. Instrum. **86**(3), 034501 (2015). https://doi.org/10.1063/1.4913660
21. R. Temirkhanova, Application of Prompt Fission Neutron Logging to the Uranium Deposits of Stratified Infiltration Type.14th Sgem Geoconference on Science and Technologies in Geology, Exploration and Mining (2014). https://doi.org/10.5593/SGEM2014%2FB11%2FS5.055
22. Z.F. Liu, C.L. Ding, R.Y. Wang et al., Current status and development trend analysis of neutron logging in uranium mines in China. J. Phys. Conf. Ser. **1865**(2), 022006 (2021). https://doi.org/10.1088/1742-6596/1865/2/022006

23. Z.F. Liu, B. Tang, Z.H. Wei et al., Correction algorithm of epithermal neutron decay time spectrum for uranium pulsed neutron logging. For. Chem. Rev. 1368–1376 (2022). www.forestchemicalsreview.com
24. J.M. Verbeke, K.N. Leung, J. Vujic, Development of a sealed-accelerator-tube neutron generator. Appl. Radiat. Isot. **53**(4–5), 801–809 (2000). https://doi.org/10.1016/S0969-8043(00)00262-1
25. L.A. Shope, R.S. Berg, M.L. O'Neal et al., The operation and life of the Zetatron neutron tube in a borehole logging application. Int. J. Appl. Radiat. Isot. **34**(1), 269–272 (1983). https://doi.org/10.1016/0020-708X(83)90130-8
26. S.J. Vala, M. Abhangi, Ratnesh Kumar et al., Development and performance of a 14-MeV neutron generator. Nucl. Instrum. Methods Phys. Res., Sect. A. **959**, 163495 (2020). https://doi.org/10.1016/j.nima.2020.163495
27. W.B. Liu, M.J. Li, K. Gao et al., Discharge characteristics of a penning ion source for compact neutron generator. Nucl. Instrum. Methods Phys. Res., Sect. A **768**, 120–123 (2014). https://doi.org/10.1016/j.nima.2014.09.052
28. W.T. Guo, S.J. Zhao, S.W. Jing et al., Effect of target film materials on neutron yield of neutron tube with drive-in target. Radiat. Phys. Chem. **182**, 109358 (2021). https://doi.org/10.1016/j.radphyschem.2021.109358
29. X.Q. Chen, L. Xiong, H. Xie et al., A high-stability neutron generator for industrial online elemental analysis. Nucl. Eng. Technol. **56**(4), 1441–1453 (2024). https://doi.org/10.1016/j.net.2023.11.048
30. B. Tang, R.B. Wang, S.M. Zhou et al., Chinese patent 201310408465. 6,13 Sep. (2013)
31. B. Tang, R.B. Wang, S.M. Zhou et al., Chinese patent 201320592725. 5,2 Apr. (2014)
32. B. Tang, H.T. Wang, R. Cheng et al., Chinese patent 201810076976. 5,6 Aug. (2018)
33. B. Tang, R.B. Wang, S.M. Zhou et al., Chinese patent 201310440359. 6,13 Sep. (2013)
34. W.W. Givens, W.R. Mills Jr., Logging technique for assaying for uranium in earth formations. United States: N. p., (1979). Web. https://www.osti.gov/biblio/5327390
35. Y. Zhang, C. Liu, S.L. Liu et al., Prompt fission neutron uranium logging(II): dead-time effect of neutron time spectrum. Nucl. Sci. Tech. **36**(2), 19 (2025). https://doi.org/10.1007/s41365-024-01615-x
36. Y. Jin, F.L. Chen, X.Y. Chai et al., Development and application of nuclear logging technique. At. Energy Sci. Technol. **38**(S1), 201–201 (2004). https://doi.org/10.7538/yzk.2004.38.S1.0201. (**in Chinese**)
37. X.F. Meng, G.S. Guo, L. Zhang et al., Neutron shielding property test with combination detection method based on moderation sphere detectors. Nucl. Sci. Tech. **39**(5), 050201 (2016). https://doi.org/10.11889/j.0253-3219.2016.hjs.39.050201
38. X.G. Wang, G.B. Wang, G.G. Zhang et al., The Monte Carlo simulation of pulsed neutron-fission neutron uranium logging technique. J. Isot. **26**(1), 48–52 (2013). https://doi.org/10.7538/tws.2013.26.01.0048
39. Y. Zhang, B. Tang, W.B. Jia et al., Application of the Monte Carlo Library Least-Squares (MCLLS) approach for chromium quantitative analysis in aqueous solution. Appl. Radiat. Isotopes **150**, 39–42 (2019). https://doi.org/10.1016/j.apradiso.2019.02.018
40. Y. Zhang, W.B. Jia, R. Gardner et al., Study on the PGNAA measurement of heavy metals in aqueous solution by the Monte Carlo Library Least-Squares (MCLLS) approach. Appl. Radiat. Isotopes **132**, 13–17 (2018). https://doi.org/10.1016/j.apradiso.2017.10.037